

Role of multiparticle-multihole states of $^{18,19}\text{O}$ in $^{18}\text{O}(n, \gamma)^{19}\text{O}$ reactions at keV energy

T. Ohsaki,^{1,*} M. Igashira,¹ Y. Nagai,^{2,3} M. Segawa,⁴ and K. Muto⁵

¹Research Laboratory for Nuclear Reactors, Tokyo Institute of Technology, 2-12-1 O-okayama, Meguro, Tokyo 152-8550, Japan

²Research Center for Nuclear Physics, Osaka University, Ibaraki, Osaka 667-0047, Japan

³Division of Nuclear Data and Reactor Engineering, Japan Atomic Energy Agency, Tokai, Ibaraki 319-1195, Japan

⁴Quantum Beam Science Directorate, Japan Atomic Energy Agency, Tokai, Ibaraki 319-1195, Japan

⁵Department of Physics, Tokyo Institute of Technology, 2-12-1 O-okayama, Meguro, Tokyo 152-8551, Japan

(Received 31 December 2006; revised manuscript received 15 October 2007; published 28 May 2008)

We have determined for the first time the partial-capture cross sections for discrete γ rays from neutron capture by ^{18}O to the $5/2^+$ ground, $1/2^+$ second, and $3/2^+$ first excited states in ^{19}O at $10 \leq E_n \leq 80$ keV. The first two cross sections agree with the calculated ones based on a nonresonant direct p -wave capture by ^{18}O within a factor of two. On the other hand, the cross section to the $3/2^+$ state with a three-particle ($d_{5/2}$)³ configuration was found to be about 180 times larger than the calculated one. We discussed a possible origin of the large discrepancy by referring to recent results of $^{18}\text{O}(n, \gamma)^{19}\text{O}$ at thermal energy.

DOI: 10.1103/PhysRevC.77.051303

PACS number(s): 25.40.Lw, 21.10.Jx, 27.20.+n, 29.30.Kv

A discrete γ ray from the neutron capture of light nuclei to low-lying states of a neutron-capturing nucleus at keV neutron energy has provided valuable information on the reaction mechanism, the nuclear structure [1–5], and the application for nuclear astrophysics [6–9]. In fact, the neutron-capture reactions of ^{12}C and ^{16}O at $10 < E_n < 80$ keV are dominated by a nonresonant direct p -wave capture process [3–5,8,9]. Intense $E1$ γ -ray strength from the reaction leading to the $1/2^+$ state of ^{13}C and ^{17}O with a large spectroscopic factor (C^2S) is much stronger than that leading to the $1/2^-$ state, as shown in Figs. 1(a) and 1(b), respectively. In the thermal-neutron capture of these nuclei, the $E1$ γ -ray strength from the reaction leading to the $1/2^-$ state is very strong [5,10,11]. Contrary to the cases for ^{12}C and ^{16}O mentioned, few γ -ray spectroscopic studies have been carried out for $^{18}\text{O}(n, \gamma)^{19}\text{O}$, although several measurements were made to observe discrete γ rays from $^{18}\text{O}(d, p\gamma)^{19}\text{O}$ [12,13], $^{17}\text{O}(t, p\gamma)^{19}\text{O}$ [13], $^2\text{H}(^{18}\text{O}, p\gamma)^{19}\text{O}$ [14] and from the β decay of ^{19}N [15]. In the recent study of $^{18}\text{O}(n, \gamma)^{19}\text{O}$ at thermal energy, the primary $E1$ γ -ray transition strength from $^{18}\text{O}(n, \gamma)^{19}\text{O}$ to the $3/2^-$ state at 3.944 MeV was found to be about 200,000 times stronger than that to the $1/2^-$ state at 3.233 MeV [16]. In addition, the $E1$ strength from the $3/2^-$ state leading to the $3/2^+$ state at 0.096 MeV with a three-particle ($d_{5/2}$)³ configuration was more than 6 times stronger than that to the $5/2^+$ ground state with a single ($d_{5/2}$) neutron, as shown in Fig. 1(c) [16]. An s -wave neutron capture by ^{18}O with a 5–10% two-hole four-particle (2h-4p) configuration with two unpaired particles, seniority 2 ($v = 2$), to the $3/2^+$ state with $v = 3$ via the sub threshold $3/2^-$ state with the 1h-4p configuration [17] with $v = 3$ could allow the observed intense $E1$ γ -ray transitions. The new observation in $^{18}\text{O}(n, \gamma)^{19}\text{O}$ at thermal energy prompted us to study the reaction at keV energy to learn

about a possible role of the mentioned multiparticle-multihole configurations of ^{18}O and ^{19}O .

Experimentally, the total cross section of $^{18}\text{O}(n, \gamma)^{19}\text{O}$, $\sigma_\gamma(^{18}\text{O})_{\text{tot.}}$, was measured by an activation method [18]. The obtained cross section, $\sigma_\gamma(^{18}\text{O})_{\text{tot.}} = 7.93 \pm 0.7 \mu\text{b}$ at $E_n = 25$ keV, agrees with the calculated value of $9.2 \mu\text{b}$ based on a nonresonant direct p -wave capture process [18]. The partial cross sections of $^{18}\text{O}(n, \gamma)^{19}\text{O}$, $\sigma_\gamma(^{18}\text{O})_{\text{part.}}$, to low-lying states of ^{19}O at keV energy were also calculated [18], but they have not yet been measured. The measurement of $\sigma_\gamma(^{18}\text{O})_{\text{part.}}$, however, is quite important to critically study the model calculation.

We used an enriched $^2\text{H}_2^{18}\text{O}$ sample (136.5 g) and a high efficiency anti-Compton NaI(Tl) spectrometer. The isotopic compositions of the $^2\text{H}_2^{18}\text{O}$ sample were as follows: 95.1% enriched in ^{18}O , 0.9% in ^{17}O , 4.0% in ^{16}O , 98.5% in ^2H , and 1.5% in ^1H . The sample was contained in a cylindrical case made of an acrylic block. It was placed 12 cm down from the ^7Li neutron production target position. A gold sample was used for normalization of the cross section, because the cross section of Au is known to have a small uncertainty of 3–5% [19]. The measurement was carried out using pulsed neutrons at $10 \leq E_n \leq 80$ keV, which were produced by the $^7\text{Li}(p, n)^7\text{Be}$ reaction. A pulsed proton beam (repetition rate of 4 MHz) was provided from the 3.2-MV Pelletron accelerator of the Research Laboratory for Nuclear Reactors at the Tokyo Institute of Technology. A neutron spectrum was measured by a ^6Li -glass scintillation counter by a time-of-flight (TOF) method [20]. Prompt γ rays from $^{18}\text{O}(n, \gamma)^{19}\text{O}$ were detected by an anti-Compton NaI(Tl) spectrometer [21], which was set at 125.3° with respect to the proton beam direction, where the second Legendre polynomial is zero. γ -ray yields detected at this angle, therefore, give the angle-integrated cross section for a dipole transition. The energy calibration of the central NaI(Tl) detector was carefully made using γ -ray standard sources, such as ^{137}Cs , ^{60}Co , and ^{88}Y , and γ rays from the β decays of ^{40}K (at 1.461 MeV) and ^{208}Tl (at 2.615 MeV), from $\text{H}(n, \gamma)^2\text{H}$ (at 2.225 MeV),

*Present address: Intellectual Property Bank Corp. 1-21-19 Toranomon, Minato, Tokyo 105-0001, Japan.

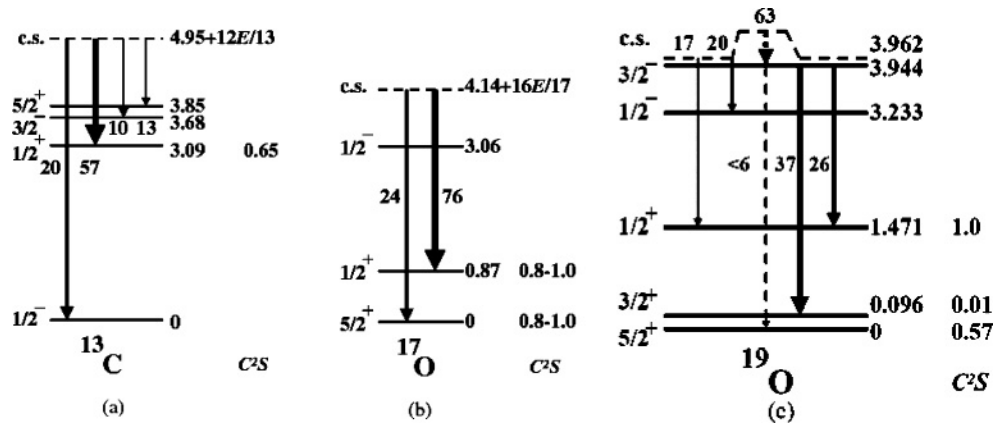


FIG. 1. Partial level schemes of ^{13}C (a), ^{17}O (b), and ^{19}O (c) are shown. The relative γ -ray intensities obtained from the neutron-capture reactions of ^{12}C (a) and ^{16}O (b) at keV energies and of ^{18}O (c) at thermal energy to low-lying states of a neutron-capturing nucleus are also shown, respectively. E and C^2S are the incident neutron energy and a spectroscopic factor, respectively.

and from $^{56}\text{Fe}(n, \gamma)^{57}\text{Fe}$ (at 4.948, 5.920, and 7.646 MeV). Consequently, the γ -ray energy from $^{18}\text{O}(n, \gamma)^{19}\text{O}$ could be determined within an uncertainty of 25 keV. Two-dimensional data on the neutron TOF and γ -ray pulse-height (PH) spectra from the anti-Compton NaI(Tl) spectrometer were stored on a personal computer in list mode. A typical TOF spectrum for a gold sample is shown in Fig. 2, where the sharp peak at channel 580 and the broad peak at channel 400 are due to γ rays from $^7\text{Li}(p, \gamma)^8\text{Be}$ at the Li neutron production target position and from $^{197}\text{Au}(n, \gamma)^{198}\text{Au}$ at keV energy, respectively. Foreground spectra including background, corresponding to the neutron energy from 30 to 80 keV, and background γ -ray spectra were obtained by putting the gates in the regions of F (foreground) and B (background) on the TOF spectrum, as shown in Figs. 3(a)–3(c). The background γ rays are due to natural radioactivities, such as that of ^{40}K , ^{208}Tl , and γ rays from the $\text{H}(n, \gamma)^2\text{H}$, the $^{56}\text{Fe}(n, \gamma)^{57}\text{Fe}$, and the $^{127}\text{I}(n, \gamma)^{128}\text{I}$

(at 6.826 MeV) reactions induced by background neutrons in the experimental room. A background-subtracted (net) γ -ray spectrum at $30 \leq E_n \leq 80$ keV was obtained as shown in Figs. 3(d)–3(f) by subtracting a background spectrum from a foreground one. In Figs. 3(d)–3(f), the solid line (bold) shows a least-squares fit of calculated response functions to the measured spectrum. The response function was calculated by convoluting the measured incident neutron spectrum to the experimental response function of the NaI(Tl) spectrometer of Refs. [20] and [21]. We see discrete γ rays of 2.25, 2.55, 3.95, and 6.30 MeV together with weak 3.09 and 3.32 MeV γ rays. Because H, ^2H , ^{12}C , and ^{16}O were contained in the $^2\text{H}_2^{18}\text{O}$ sample and/or in a sample case made of an acrylic block, the 2.25 and 6.30 MeV γ rays were identified to be from $\text{H}(n, \gamma)^2\text{H}$ and $^2\text{H}(n, \gamma)^3\text{H}$, respectively. The 2.25 MeV γ -ray spectrum are well reproduced by the calculated response function, as shown in Fig. 3(f). The 3.09 and 3.32 MeV γ rays were due to the $^{12}\text{C}(n, \gamma)^{13}\text{C}$ and $^{16}\text{O}(n, \gamma)^{17}\text{O}$ reactions leading to the $1/2^+$ state of ^{13}C and ^{17}O , respectively [8,9]. The 3.95 MeV γ -ray line was analyzed as follows. In the present study, one observed around 4 MeV the 4.01 and 3.92 MeV γ rays, direct transitions to the $5/2^+$ ground and the $3/2^+$ state at 0.096 MeV, respectively, and the 3.85 MeV cascade transition from the $3/2^-$ state at 3.94 MeV to the $3/2^+$ state, which was observed in thermal-neutron capture of ^{18}O [16]. Hence, the present analysis was carried out by making a least-squares fit of the calculated response functions to the measured spectrum in the following three cases. The response functions were calculated by convoluting the response function of the 3.85, 3.92, and 4.01 MeV γ rays (case A) and of the 3.92 and 4.01 MeV γ rays (case B). The response function for the single 3.92 MeV γ ray was used (case C). The fitted spectra for the cases A, B, and C are shown in Fig. 3(e) as solid (thin), bold solid, and dotted curves, respectively, and the reduced χ squares are 0.82 (A), 0.23 (B), and 0.77 (C), respectively. The best fit was obtained in case B, in which the intensities of the 3.92 and 4.01 MeV γ rays were given to be 70 ± 17 and $30 \pm 15\%$, respectively. The obtained intensities for the 3.85, 3.92, and 4.01 MeV

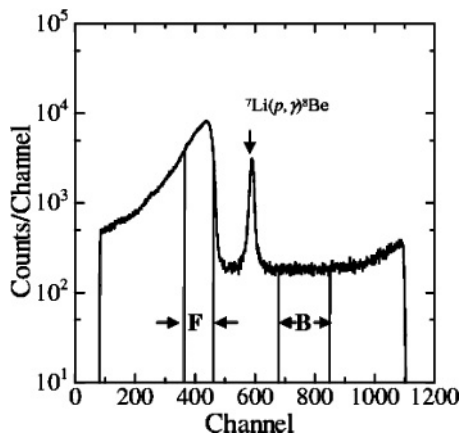


FIG. 2. Time-of-flight spectrum measured by the NaI(Tl) detector for a gold sample. The sharp peak at channel 580 is due to γ -rays from $^7\text{Li}(p, \gamma)^8\text{Be}$ and the broad peak at channel 400 is due to the keV neutron capture by Au. Here “F” and “B” show the gate position to obtain foreground spectra including background, and background γ -ray spectra, respectively.

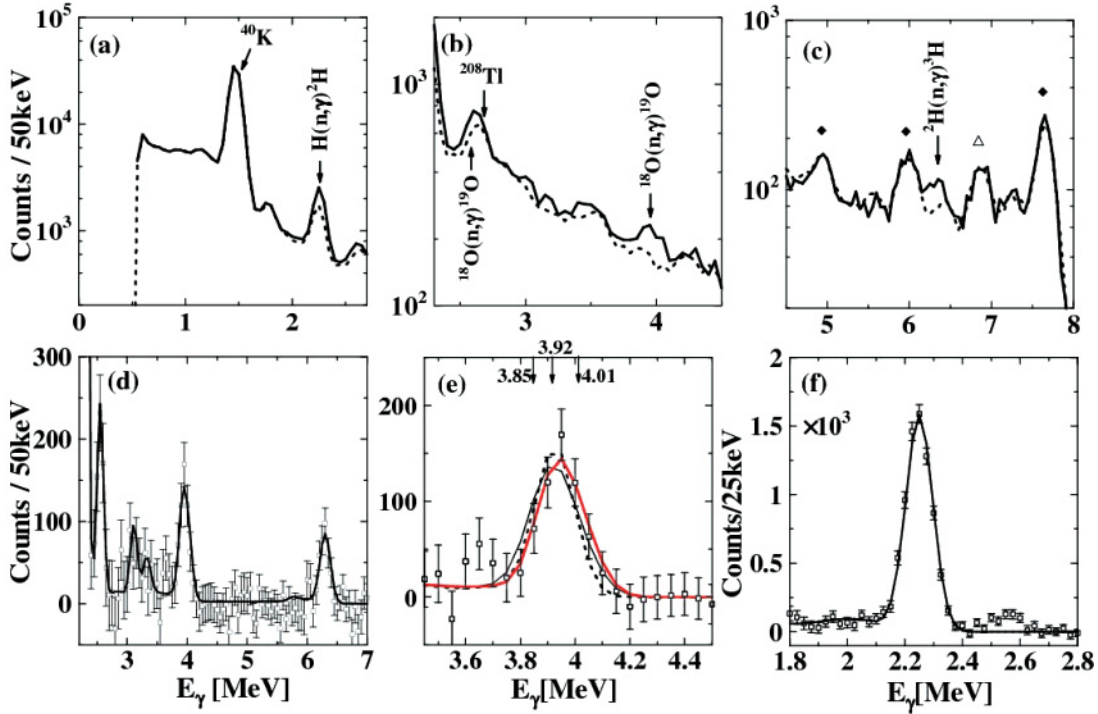


FIG. 3. (Color online) (a)–(c) Foreground (solid line) and background (dotted line) γ -ray spectra for the neutron capture by ${}^2\text{H}_2{}^{18}\text{O}$. Background γ rays are due to activities of ${}^{40}\text{K}$, ${}^{208}\text{Tl}$, and γ rays from $\text{H}(n, \gamma){}^2\text{H}$, ${}^{56}\text{Fe}(n, \gamma){}^{57}\text{Fe}$ (filled diamonds), and ${}^{127}\text{I}(n, \gamma){}^{128}\text{I}$ (open triangle). In the net γ -ray spectra (d)–(f), least-squares fits of the calculated response functions to the experimental data (open circles) are shown as solid curves (bold). In (d), the 2.55, 3.92, and 4.01 MeV γ rays are primary transitions from ${}^{18}\text{O}(n, \gamma){}^{19}\text{O}$ to $1/2^+$, $3/2^+$, and $5/2^+$ states of ${}^{19}\text{O}$, respectively. The 3.09 and 3.32 MeV γ rays are from ${}^{12}\text{C}(n, \gamma){}^{13}\text{C}$ and ${}^{16}\text{O}(n, \gamma){}^{17}\text{O}$ to the $1/2^+$ state of ${}^{13}\text{C}$ and ${}^{17}\text{O}$, respectively. The 2.25 MeV γ ray in (f) and the 6.30 MeV γ ray in (d) are from $\text{H}(n, \gamma){}^2\text{H}$ and ${}^2\text{H}(n, \gamma){}^3\text{H}$, respectively. In (e), least-squares fits of the calculated response functions to the measured spectrum are shown. The response functions were obtained by convoluting the response function of the 3.85, 3.92, and 4.01 MeV γ rays (thin curve) and of the 3.92 and 4.01 MeV γ rays (solid bold curve). The response function for the 3.92 MeV γ ray was also used (dotted curve). The solid bold curve is shown to give the best fit to the measured spectrum.

γ rays were 20, 60, and 20%, respectively (case A). Because of the poor quality of the fit for the case A compared to the fit for the case B, the 3.85 MeV γ -ray intensity was considered to be less than 20% of the measured 3.95 MeV one. Similar to the case mentioned, the 2.55 MeV line was fitted well by the response function mentioned. Consequently, the 2.55, 3.92, and 4.01 MeV γ rays were identified as primary transitions from ${}^{18}\text{O}(n, \gamma){}^{19}\text{O}$ to $1/2^+$, $3/2^+$, and $5/2^+$ states of ${}^{19}\text{O}$, respectively.

The 2.55, 3.09, 3.32, 3.92, 4.01, and 6.30 MeV γ -ray yields in the net spectrum were obtained using the response function mentioned. Using the obtained γ -ray yield for the i th γ -ray transition with energy E_i from ${}^{18}\text{O}(n, \gamma){}^{19}\text{O}$ to the low-lying state i , $Y_{\gamma, E_i}({}^{18}\text{O})$ [or for the γ -ray transition from ${}^2\text{H}(n, \gamma){}^3\text{H}$, $Y_{\gamma}({}^2\text{H})$], the partial capture cross section, $\sigma_{\gamma}({}^{18}\text{O})_i$, corresponding to the i th γ -ray transition [or the capture cross-section $\sigma_{\gamma}({}^2\text{H})$] is given by

$$\sigma_{\gamma}(A)_i = \frac{T_{\text{Au}}}{T_A} \frac{P_A}{P_{\text{Au}}} \frac{C_{\text{Au}}}{C_A} \cdot \frac{(r^2 n)_{\text{Au}}}{(r^2 n)_A} \frac{Y_{\gamma, i}(A)}{Y_{\gamma}(A)} \cdot \sigma_{\gamma}(A). \quad (1)$$

Here, A stands for ${}^{18}\text{O}$ or ${}^2\text{H}$, and Au refers to ${}^{197}\text{Au}$. $T_{\text{Au}}(T_A)$ and $P_{\text{Au}}(P_A)$ are the number of the neutron counts measured by the ${}^6\text{Li}$ -glass detector during the measurements

of gold (a sample A), and the neutron transmission of a gold sample, respectively; r and n are the radius and thickness (atoms/barn) of the sample, respectively; and $Y_{\gamma}(\text{Au})$ and $\sigma_{\gamma}(\text{Au})$ are the γ -ray yield and the absolute capture cross section for Au, respectively. A correction factor C_{Au} is introduced to correct for the overestimation of the γ -ray yield due to the multiple-scattering effect of, and of the shielding of the incident neutrons in a sample, respectively, and was calculated using a Monte-Carlo code, TIME-MULTI [22]. The present $\sigma_{\gamma}({}^2\text{H})$ of $1.9 \pm 0.3 \mu\text{b}$ and $\sigma_{\gamma}({}^{12}\text{C})_{1/2}^+$ of $11 \pm 3 \mu\text{b}$ at $E_n = 52$ keV are in good agreement with previous results of $1.99 \pm 0.25 \mu\text{b}$ at $E_n = 54.2$ keV [23] and of $8.6 \pm 1.1 \mu\text{b}$ at $E_n = 50$ keV [8], respectively. The partial cross sections for the γ -ray transitions from ${}^{18}\text{O}(n, \gamma){}^{19}\text{O}$ to the $1/2^+$ state, $\sigma_{\gamma}({}^{18}\text{O})_{1/2}^+$, the $3/2^+$ state, $\sigma_{\gamma}({}^{18}\text{O})_{3/2}^+$, and the $5/2^+$ state, $\sigma_{\gamma}({}^{18}\text{O})_{5/2}^+$, were determined for the first time, as given in Table I, together with the calculated values in Ref. [18]. The quoted uncertainty (Table I) is the result of combined uncertainties of the γ -ray yield statistics, the absolute cross section of Au (3%) the response function of the NaI(Tl) spectrometer (2%), and the correction factor (3%). The total cross section $\sigma_{\gamma}({}^{18}\text{O})_{\text{tot.}}$, $9.8 \pm 1.4 \mu\text{b}$ at $E_n = 52$ keV, agrees with the value of $11.4 \pm 1.0 \mu\text{b}$ obtained by extrapolating the previous value of $7.93 \pm 0.7 \mu\text{b}$ at $E_n =$

TABLE I. Measured and calculated [18] partial and total cross sections of the $^{18}\text{O}(n, \gamma)^{19}\text{O}$ reaction (in units of μb) at the average neutron energy 52 keV.

E_γ (MeV)	Placement	$\sigma(n, \gamma)$		E_γ (MeV)	Placement	$\sigma(n, \gamma)$	
		Exp.	Cal.			Exp.	Cal.
4.01 ± 0.025	c.s. $\rightarrow 0$	1.6 ± 0.8	2.0	3.85	$3.94 \rightarrow 0.096$	<1.0	0.04
3.92 ± 0.025	c.s. $\rightarrow 0.096$	3.6 ± 0.9	0.02				
2.54 ± 0.025	c.s. $\rightarrow 1.471$	4.6 ± 0.8	10				
	Total	9.8 ± 1.4	12				

25 keV to 52 keV within the experimental uncertainty [18]. The obtained $\sigma_\gamma(^{18}\text{O})_{1/2}^+$ of $4.6 \pm 0.8 \mu\text{b}$ and $\sigma_\gamma(^{18}\text{O})_{5/2}^+$ of $1.6 \pm 0.8 \mu\text{b}$ agree with the calculated ones of 10 and $2.1 \mu\text{b}$ within a factor of two. The $\sigma_\gamma(^{18}\text{O})_{3/2}^+$ of $3.6 \pm 0.9 \mu\text{b}$, however, is about 180 times larger than the calculated one of about $0.02 \mu\text{b}$ [18]. Here, it should be mentioned that the nucleosynthetic yield of light nuclei in stars has been estimated by taking into account such a nonresonant p -wave capture process [24]. It is, therefore, very important to understand the origin of the anomalously large $\sigma_\gamma(^{18}\text{O})_{3/2}^+$ to calculate the neutron capture cross section of a nucleus at stellar temperature, corresponding to the neutron energy from a few to a few hundred keV.

Here it is worth mentioning that the $J^\pi = 3/2^-$ resonance state at 4.58 MeV has been estimated to contribute little to the $\sigma_\gamma(^{18}\text{O})_{3/2}^+$ at $E_n \approx 52$ keV, about $0.01 \mu\text{b}$ [18]. The contribution of the s -wave neutron capture process to the present cross section of $\sigma_\gamma(^{18}\text{O})_{3/2}^+$ is also negligibly small. Actually, the partial cross section for the 3.85 MeV γ -ray transition from the neutron capture to the $3/2^+$ state via the $3/2^-$ state was estimated to be $0.038 \mu\text{b}$ by extrapolating the measured thermal capture cross section to 52 keV by assuming a $1/v$ law [18] and by using the measured γ -ray branching ratio for the 3.85 MeV γ ray at thermal energy [16]. Therefore, one would expect a significant contribution due to the nonresonant p -wave capture process to the obtained $\sigma_\gamma(^{18}\text{O})_{3/2}^+$, and we reconsidered the calculated cross section $\sigma_\gamma(^{18}\text{O})_{3/2}^+$ of $0.02 \mu\text{b}$ [18]. The calculation was made using a small spectroscopic factor (C^2S) of 0.01 obtained by $^{18}\text{O}(d, p)^{19}\text{O}$ [16,18]. To get a deeper insight of the present large $\sigma_\gamma(^{18}\text{O})_{3/2}^+$, therefore, we note the intense $E1$ γ -ray strength from $^{18}\text{O}(n, \gamma)^{19}\text{O}$ to $3/2^+$ via the $3/2^-$ state at 3.94 MeV at thermal energy. The $3/2^-$ subthreshold state at 3.94 MeV has the $1h$ - $4p$ configuration, as mentioned above. Here, it is noteworthy that, according to theoretical calculations using a modification of the Millener-Kurath interaction [17] and/or the WBN interaction of Warburton and Brown [18], a number of $J^\pi = 1/2^-$ and $3/2^-$ states, which are described as a linear combination of a $1h$ - $4p$ configuration with $1\hbar \omega$ excitation, have been predicted in an energy region around the neutron threshold of ^{19}O [18]. Hence, similar to the case for thermal neutron (s -wave) capture by ^{18}O with the $2h$ - $4p$ configuration to $3/2^+$ mentioned [16], the large cross section $\sigma_\gamma(^{18}\text{O})_{3/2}^+$ could be attributed to a p -wave neutron capture of ^{18}O with the $2h$ - $4p$ configuration to $3/2^+$ with $v = 3$ through an intermediate negative-parity $1/2^-$ and $3/2^-$ state with the $1h$ - $4p$ configuration with $v = 3$ in ^{19}O . Such

negative-parity states could be populated by a p -wave neutron capture of ^{18}O , and an $E1$ γ -transition from the populated states could reach the $3/2^+$ state with $v = 3$, as follows. Here, we only describe the nuclear configurations of ^{18}O and ^{19}O , which are relevant to the $E1$ transition following the nonresonant p -wave neutron-capture reaction by ^{18}O at keV energy.

The ground state of ^{18}O consists mainly of two neutrons outside the core of ^{16}O and of the 5–10% $2h$ - $4p$ component, as given below. Here, $a, b, c, d, e, f, g, h, i, j, k,$ and ℓ are numerical coefficients that determine the amount of each wave function in each nuclear state:

$$|0^+\rangle = a|(sd)_{J=0}^2\rangle + b|(p)_{J=0}^{-2}(sd)_{J=0}^4\rangle + c|(p)_{J=2}^{-2}(sd)_{J=2}^4\rangle. \quad (2)$$

Nonresonant direct p -wave neutron capture by ^{18}O leads to the following configurations as a scattering state |c.s.):

$$|\text{c.s.}\rangle = d|n \otimes (sd)_{J=0}^2\rangle + e|n \otimes (p)_{J=0}^{-2}(sd)_{J=0}^4\rangle + f|n \otimes (p)_{J=2}^{-2}(sd)_{J=2}^4\rangle. \quad (3)$$

Here, the second and third states are $2h$ - $5p$ states with $3\hbar \omega$ excitation with respect to low-lying positive-parity states of ^{19}O . The unperturbed energies of these configurations would be in a much higher excitation energy region than the neutron threshold, and thus the coefficients e and f are small in the scattering states with $J^\pi = 1/2^-$ and $3/2^-$.

The main components of the ground $5/2^+$ and excited $1/2^+$ (at 1.472 MeV) states are of a single-particle character, as described below:

$$|5/2^+\rangle = g|(d_{5/2})_{v=1}^3\rangle, \quad (4)$$

$$|1/2^+\rangle = h|(d_{5/2})_{v=0, J=0}^2(s_{1/2})^1\rangle. \quad (5)$$

The $3/2^+$ state at 0.096 MeV is a three-particle ($v = 3$) state, as given below:

$$|3/2^+\rangle = i|(d_{5/2})_{v=3}^3\rangle + j|(d_{5/2})_{v=2, J=2}^2(s_{1/2})^1\rangle, \quad (6)$$

where v denotes a seniority quantum number, which is equal to the number of unpaired neutrons. The nonresonant p -wave neutron capture by ^{18}O leads to the ground $5/2^+$ and excited $1/2^+$ states, respectively, by emitting $E1$ radiation, as described above. The three-particle ($v = 3$) $3/2^+$ state, however, cannot be reached by an $E1$ γ -ray transition from a scattering state with $v = 1$ by a nonresonant p -wave capture of the ^{18}O ground state with $v = 0$, as demonstrated in the calculated small cross section.

According to the calculations of the mentioned negative-parity states, the wave functions are 1h-4p excitations mostly from the full p into the sd shell [17,18]. Hence, the lowest order configurations, for negative-parity states in ^{18}O , may be expressed as

$$|1/2^-(3/2^-)\rangle = k|(p)^{-1}(sd)_{J=0}^4\rangle + l|(p)^{-1}(sd)_{J=2}^4\rangle. \quad (7)$$

These states could be excited as an intermediate state via nuclear interactions of incident p -wave neutrons with the ^{18}O ground state with the 2h-4p component, as described below. The first part of Eq. (7) cannot contribute to reaching the $J^\pi = 3/2^+$ state via an $E1$ γ transition, because four neutrons in the sd shell have seniority $v = 0$ and a single-particle transition, such as $d_{5/2} \rightarrow p_{3/2}$, and/or $s_{1/2} \rightarrow p_{1/2}, p_{3/2}$, of the $E1$ decay cannot leave $v = 3$ components in the sd shell. The second part with $v = 2$ components in the sd shell, however, is contributing to the population of the $J^\pi = 3/2^+$ state with $v = 3$ via an $E1$ γ transition through a single-particle transition $d_{5/2} \rightarrow p_{3/2}$.

$$\begin{aligned} &\langle (d_{5/2})_{v=3, J=3/2}^3 | E1 | (p)^{-1}(sd)_{J=2}^4 \rangle \langle (p)^{-1}(sd)_{J=2}^4 | H_{\text{int}} \\ &\times | n \otimes (p)_{J=2}^{-2}(sd)_{J=2}^4 \rangle \end{aligned} \quad (8)$$

Here, H_{int} is a nuclear interaction that produces a mixing of the states, and the incoming neutron n is in a p state. The comparison of the measured $\sigma_\gamma(^{18}\text{O})_{3/2}^+$ to a calculated one based on the mentioned process is extremely interesting, but is beyond the present study.

In summary, we found that the partial neutron-capture cross sections of ^{18}O to the $1/2^+$ and $5/2^+$ states agree with the calculated ones on the basis of a nonresonant p -wave capture process within a factor of two. The cross section to the $3/2^+$ state with the three $(d_{5/2})^3$ neutrons, however, is about 180 times larger than the calculated one. The large cross section could be interpreted qualitatively as being due to a p -wave neutron capture of ^{18}O with $v = 2$ to the $3/2^+$ state with $v = 3$ via $3/2^-$ and/or $1/2^-$ states with a 1h-4p configuration with $v = 3$.

We thank H. Ohtsubo, K. Matsuyanagi, and A. Volya for useful discussions and T. Matsumoto, K. Mishima, K. Saito, K. Ohgama, and J. Nishiyama for their help in the experiment. We thank K. Tosaka for reliable operation of the Pelletron accelerator. This work was supported by a Grant-in-Aid for Scientific Research of the Japan Ministry of Education, Culture, Sports, Science, and Technology.

-
- [1] A. M. Lane and J. E. Lynn, Nucl. Phys. **17**, 563 (1960).
 [2] S. Raman, M. Igashira, Y. Dozono, H. Kitazawa, M. Mizumoto, and J. E. Lynn, Phys. Rev. C **41**, 458 (1990).
 [3] Y. K. Ho, H. Kitazawa, and M. Igashira, Phys. Rev. C **44**, 1148 (1991).
 [4] T. Otsuka, M. Ishihara, N. Fukunishi, T. Nakamura, and M. Yokoyama, Phys. Rev. C **49**, R2289 (1994); A. Mengoni, T. Otsuka, and M. Ishihara, *ibid.* **52**, R2334 (1995).
 [5] T. Kikuchi, Y. Nagai, T. S. Suzuki, T. Shima, T. Kii, M. Igashira, A. Mengoni, and T. Otsuka, Phys. Rev. C **57**, 2724 (1998).
 [6] R. R. Winters and R. L. Macklin, Astrophys. J. **329**, 943 (1988).
 [7] H. Beer, G. Rupp, F. Voss, and F. Keappeler, Astrophys. J. **79**, 420 (1991).
 [8] Y. Nagai, M. Igashira, K. Takeda, N. Mukai, S. Motoyama, F. Uesawa, H. Kitazawa, and T. Fukuda, Astrophys. J. **372**, 683 (1991); T. Ohsaki, Y. Nagai, M. Igashira, T. Shima, K. Takeda, S. Seino, and T. Irie, *ibid.* **422**, 912 (1994).
 [9] M. Igashira, Y. Nagai, K. Masuda, T. Ohsaki, and H. Kitazawa, Astrophys. J. **441**, L89 (1995).
 [10] E. T. Jurney, P. J. Bendt, and J. C. Browne, Phys. Rev. C **25**, 2810 (1982).
 [11] A. B. McDonald *et al.*, Nucl. Phys. **A281**, 325 (1977).
 [12] P. Fintz, F. Hibou, B. Rastegar, and A. Gallmann, Nucl. Phys. **A150**, 49 (1970).
 [13] F. Hibou, P. Fintz, B. Rastegar, and A. Gallmann, Nucl. Phys. **A171**, 603 (1971).
 [14] C. Broude, U. Karfunkel, and Y. Wolfson, Nucl. Phys. **A161**, 241 (1971).
 [15] C. S. Sumithrarachchi, D. W. Anthony, P. A. Lofy, and D. J. Morrissey, Phys. Rev. C **74**, 024322 (2006).
 [16] Y. Nagai, M. Segawa, T. Ohsaki, H. Matsue, and K. Muto, Phys. Rev. C **76**, 051301(R) (2007).
 [17] E. K. Warburton, Phys. Rev. C **38**, 935 (1988); E. K. Warburton and B. A. Brown, Phys. Rev. C **46**, 923 (1992).
 [18] J. Meissner, H. Schatz, J. Gorres, H. Herndl, M. Wiescher, H. Beer, and F. Kappeler, Phys. Rev. C **53**, 459 (1996).
 [19] ENDF/B-VI data file for ^{197}Au (MAT = 7925), evaluated by P. G. Young (1984).
 [20] Y. Nagai, T. S. Suzuki, T. Kikuchi, T. Shima, T. Kii, H. Sato, and M. Igashira, Phys. Rev. C **56**, 3173 (1997).
 [21] M. Igashira, K. Tanaka, and K. Masuda *et al.*, *Proceedings of the Conference of the 8th International Symposium on Capture γ Ray Spectroscopy and Related Topics, Fribourg, Switzerland, 1993*, edited by J. Kern (World Scientific, Singapore, 1994), p. 992.
 [22] K. Senoo, Y. Nagai, T. Shima, T. Ohsaki, and M. Igashira, Nucl. Instrum. Methods A **339**, 556 (1994).
 [23] Y. Nagai, T. Kobayashi, T. Shima, T. Kikuchi, K. Takaoka, M. Igashira, J. Golak, R. Skibinski, H. Witala, A. Nogga, W. Glockle, and H. Kamada, Phys. Rev. C **74**, 025804 (2006).
 [24] R. Gallino, C. Arlandini, M. Busso, M. Lugaro, C. Travaglio, O. Straniero, A. Chieffi, and M. Limongi, Astrophys. J. **497**, 388 (1998); M. Rayet and M. Hashimoto, Astron. Astrophys. **354**, 740 (2000); C. Travaglio, R. Gallino, E. Arnone, J. Cowan, F. Jordan, and C. Sneden, Astrophys. J. **601**, 864 (2004); T. Sasaqui, T. Kajino, G. J. Mathews, K. Otsuki, and T. Nakamura, *ibid.* **634**, 1173 (2005); L. S. The, M. F. El Eid, and B. S. Meyer, *ibid.* **655**, 1058T (2007).